COMPUTER SIMULATION OF HIGH-CURRENT DIODE: FROM FIELD EMISSION TO SPACE CHARGE LIMITED CURRENT FLOW

O.V. Manuilenko, V.I. Karas', E.A. Kornilov, V.A. Vinokurov, V.S. Antipov
National Science Center "Kharkov Institute of Physics and Technology", Kharkov, Ukraine
E-mail: ovm@kipt.kharkov.ua

The results of numerical simulation of electron beam dynamics in the high-current diode with a blade-like cathode, which operates in the field emission regime, are presented. The computer simulations were performed by particle-in-cell method in the electrostatic approximation. It is shown that there are two modes of diode operation. In the first operation mode the space charge in the diode gap insignificant. In this case the anode current is small, and its value is determined by the Fowler-Nordheim law. This mode, with increasing potential difference between the cathode and the anode, passes in a mode of the space charge limited diode current. In this case the anode current is determined by the Child-Langmuir law. It is shown that the electron energy distribution function at the anode is almost monochromatic, with a maximum, which is determined by the potential difference between the cathode and the anode. The spatial electron distribution function is significantly expanded compared with the thickness of the cathode due to the topography of the electric field and space charge forces.

PACS: 41.75.-i, 52.40.Mj, 52.58.Hm, 52.59.-f, 52.65.Rr

INTRODUCTION

The usage of linear induction accelerators (LIA) for obtaining high-current ion beams (HCIBs) with the parameters required for different applications – from heavy-ion fusion up to surface modification and radiation materials science – is perspective, as LIA can operate at high pulse frequency, and can accelerate HCIBs of virtually any ions, and perform time compression of current pulse in the acceleration process, which eliminates the operations related to the increase of current due to compression rings. Collective focusing techniques can significantly increase the ion beam current. In such kind of LIA, the ion beam space charge is compensated by electrons, and the electron current is suppressed by magnetic insulation of accelerating gaps [1, 2]. The mechanism for charge and current neutralization of an HCIB by an electron beam in an axisymmetric accelerating gap was investigated in [2 - 4]. The transportation, acceleration and stability of compensated ion beam in the 1-6 cusps were studied in [5 - 7]. The transportation and acceleration of the neutralized high-current ion bunch with additional compensation of the accelerated ion bunch space charge by thermal electrons were studied in [8, 9].

The charge and current neutralization of the HCIB by the electron beam requires electron beams with energies up to 10 MeV and currents up to 20 kA. The energy and current of the electron beam should be controlled independently. These currents can be generated by a high-current diode with a knife-like cathode which works in the regime of the field- or explosive emission. The diode shape for HCIB neutralization in LIA is different from the usual. It consists of a thin ring, which is a blade-like cathode (Fig. 3). Cylindrical anode having a radius less than the inner radius of the cathode is inserted into the cathode. This structure is placed in a cylindrical vacuum chamber. According to our experiments, at applying a negative voltage to the cathode ~ 100…200 kV, in this system the electron beam is generated with a current of about 5…10 kA. Analytical theory for the high-current diodes of this shape does not exist at the moment, and the experimental data are limited.

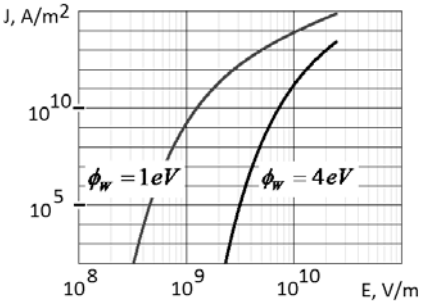

Fig. 1. The field emission current density as a function of the electric field for ϕ_W=1 eV – barium oxide, barium on tungsten substrate, and ϕ_W =4 eV – tungsten, iron. $\beta_{FN} = 1$

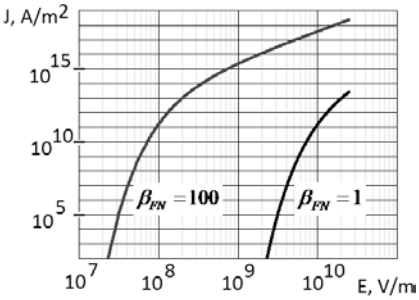

Fig. 2. The field emission current density as a function of the electric field for $\beta_{FN} = 1$ and $\beta_{FN} = 100$. $\phi_W = 4$ eV

Therefore, the diode was investigated numerically by particles-in-cell method in the electrostatic approximation with the XOOPIC code [10]. In the numerical simulations below, we assume that the electron beam is generated as a result of field emission, which is defined by the Fowler-Nordheim law [11, 12]:

$$J_{FN} = 1.54 \cdot 10^{-6} \frac{(\beta_{FN} E)^2}{\phi_W \eta^2(y)} \exp\left(-6.83 \cdot 10^9 \frac{\phi_W^{3/2}}{\beta_{FN} E} \theta(y) \right),$$

where J_{FN} is the current density, SI units, $y = 3.79 \cdot 10^{-5} \sqrt{E} / \phi_W$; E is the electric field strength on the cathode; SI units; $\eta(y) \approx 1.0$, it slightly varies with y; $\theta(y) = 1 - C_V y^2$ – Nordheim function [12], in the simulations below $C_V = 0$, functions $\eta(y)$ and

$\theta(y)$ are tabulated [13, 14], ϕ_W – work function, β_{FN} – field enhancement factor. The current density J_{FN} depends strongly on the cathode material, i.e. the work function ϕ_W (Fig. 1), and the cathode surface quality, i.e., the field enhancement factor β_{FN} (Fig. 2). The field enhancement factor for conventional cathodes ranges from 10 to 300 [15].

COMPUTER SIMULATION RESULTS

Fig. 3 shows the axially symmetric simulation domain, where rA is the outer radius of the anode, rA = 0.5 cm, rL is the outer radius of the cathode, rL = 2.5 cm, zL is the length of the simulation domain along the longitudinal axis, zL = 4 cm. The cylindrical blade-like cathode is located in the middle of the computational domain. The inner radius of the cathode rC = 1.5 cm, its thickness δ = 0.2 mm. The negative electrical potential V_C is applied to the cathode, the anode is grounded. Electrons are injected into the computational domain as a result of field emission in accordance with the Fowler-Nordheim law both the face of the cathode and its side surfaces. The outer boundary of the computational domain $r = rL$ is a metal, which is under the cathode potential V_C. The left (z = 0) and right (z = zL) boundaries of the computational domain are dielectrics. The particles that hit the border of the simulation domain are absorbed. The numerical simulations, which are presented below, performed for β_{FN} = 100 and V_C from -75 up to -300 kV.

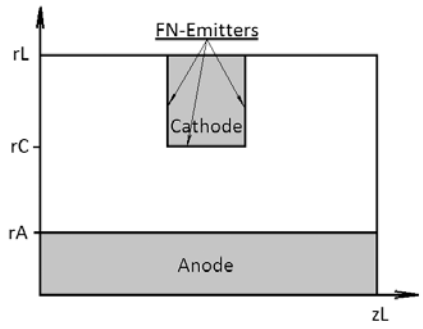

Fig. 3. The simulation domain

Figs. 4, 5 show the distributions of the electric potential $V(r,z)$ and the electric fields $E_r(r,z)$ in the computational domain for V_C = {-75, -150, -300} kV at a time that is significantly greater than the electron transit time through the diode gap, i.e. when the system "electron beam – diode gap" is in equilibrium. As seen in Figs. 4, 5, with the growth of the cathode potential, the space charge is accumulated in the diode gap, which shields the "vacuum" electric field of the cathode.

Fig. 6 shows the distribution of the electrons in the configuration space {r, z} for V_C . = {-75, -150, -300} kV at the time when the "electron beam – diode gap" system is in equilibrium. The increasing cathode potential results in an increase of the longitudinal dimension of the beam at the anode. Fig. 6 also shows that at steady state electron emission occurs, mainly, with the end of the cathode, while in the initial time interval, when in the diode are not a lot of electrons, emission takes place from the side surfaces of the anode which are close to the end face of the cathode.

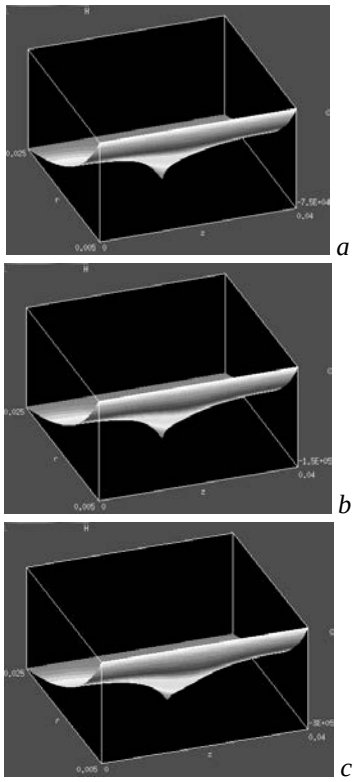

Fig. 4. The electric potential $V(r,z)$ in the diode: V_C = -75 kV (a); V_C = -150 kV(b); V_C = -300 kV(c)

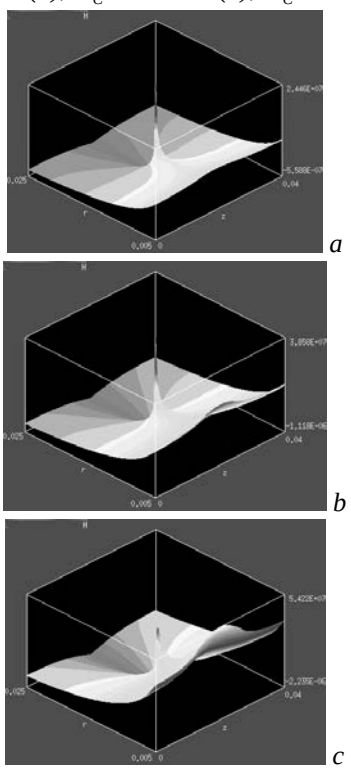

Fig. 5. The electric field $E_r(r,z)$ in the diode: V_C = -75 kV (a); V_C = -150 kV (b); V_C = -300 kV (c)

The bunching of the electron beam, which can be seen in the Fig. 6,c, can be attributed to over-voltage of the diode gap, which leads to the explosive growth of

the electron emission from the cathode surface and rapid screening of the initial "vacuum" electric field on the surface of the cathode by the space charge of the electron cloud, further rapid displacement of electrons toward the anode, which is leads to the unscreening of the cathode electric field, which in turn again leads to an explosive growth of emission from the cathode surface and the process repeated.

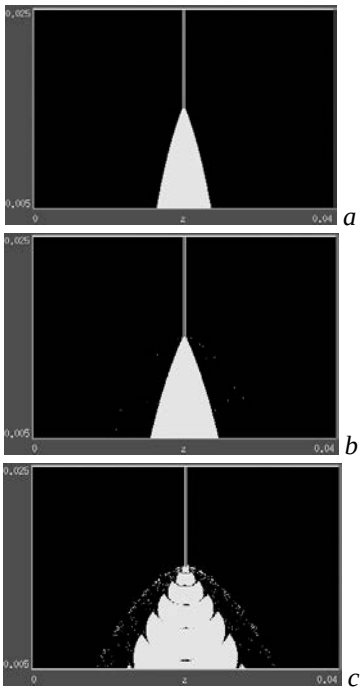

Fig. 6. The distribution of the electrons in the configuration space {r, z}: V_C = -75 kV (a); V_C = -150 kV (b); V_C = -300 kV (c)

Fig. 7, as an example, shows the electron distribution on the anode surface as function of energy and longitudinal coordinate at V_C = -75 kV. It is seen that the electron energy distribution function is almost monochromatic, with a maximum which is determined by the cathode potential V_C, in this case ~ 75 keV. This behavior of the electron energy distribution function, depending on the cathode potential, is maintained for all studied potentials. The distribution function in the longitudinal direction significantly broadened in comparison with the thickness of the cathode. This is due to the topography of the electric field at the cathode, and the influence of the space charge.

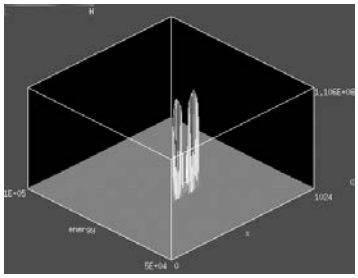

Fig. 7. The electron distribution on the anode surface as function of energy and longitudinal coordinate

Fig. 8 shows, as a function of time, the anode current $I_A(t)$ (left column) and the cathode electric field in the its center $E_r(t)$ (right column) at different applied cathode voltages.

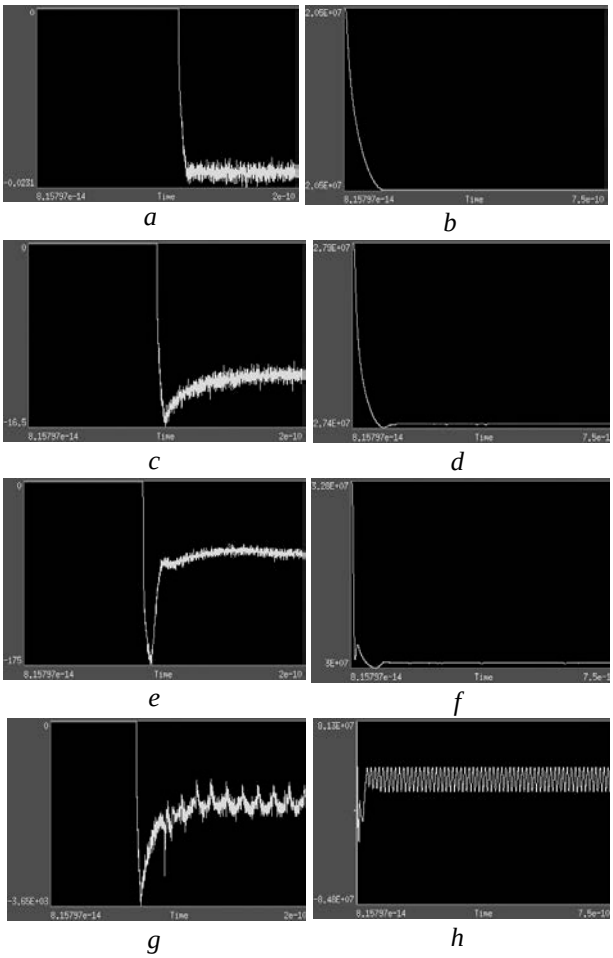

Fig. 8. The anode current $I_A(t)$ (a, c, e, g) and the cathode electric field $E_r(t)$ (b, d, f, h) vs time: V_C = -75 kV (a, b); V_C = -102 kV (c, d); V_C = -120 kV (e, f); V_C = -300 kV (g, h)

As seen in Fig. 8, regardless of the cathode potential, after the start of the field emission, electric field at the cathode surface is reduced due to the occurrence of a negative space charge in the diode gap, which leads to the suppression of electron emission. If the applied voltage V_C = {-75, -102} kV, the decreasing of the electric field is insignificantly. When the front of emitted electrons reaches the anode, the electric field at the cathode takes its self consistent steady-state value. The stationary value of the cathode electric field is slightly different from the minimal field at the cathode. The field at the cathode is minimized when the front of emitted electrons crosses the plane of the anode. This mode of diode operation corresponds to the case, when the space charge in the diode gap is insignificant. The current at the anode is determined by the Fowler-Nordheim law. If the applied potential V_C = {-120, -300} kV, then after the front of emitted electrons reaches the anode, the electric field at the cathode significantly increases as compared with the minimal electric field at the cathode, but remains lower than the initial “vacuum” field. This increase in the cathode electric field, compared to the minimal cathode field, is due to the fact that the flow of electrons through the anode is greater than the flow of

injection of electrons into the diode gap due to field emission. The effect of the space charge on the anode current is significant in this mode of diode operation. The diode current in this operation mode is limited by the space charge.

Fig. 9 shows the maximal current $I_{\max}(V_C)$ and the steady-state/averaged $I_{ave}(V_C)$ current at the anode depending on the applied cathode voltage. The data for Fig. 9 are taken from the Fig. 8. It can be seen that when the space charge is not significant ($|V_C|$ < 120 kV), the maximal and steady-state currents are practically the same. In diode operation mode, when its current is limited by the space charge ($|V_C|$ > 120 kV) $I_{\max}(V_C) > I_{ave}(V_C)$.

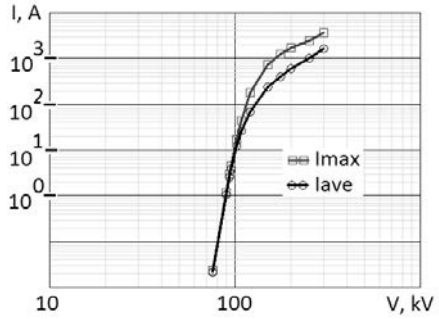

Fig. 9. The $I_{\max}(V_C)$ and the $I_{ave}(V_C)$ at the anode depending on the applied cathode voltage

Fig. 10 shows the steady-state/averaged current density $J_{ave}(V_C)$ as a function of the cathode applied voltage V_C. In addition, Fig. 10 shows an approximation of the $J_{ave}(V_C)$ by the Fowler-Nordheim law and the Child-Langmuir law. As can be seen from the Fig. 9, when $|V_C|$ < 120 kV, the $J_{ave}(V_C)$ is quite well approximated by the Fowler-Nordheim law, otherwise ($|V_C|$ > 120 kV) the $J_{ave}(V_C)$ is quite well approximated by the Child-Langmuir law.

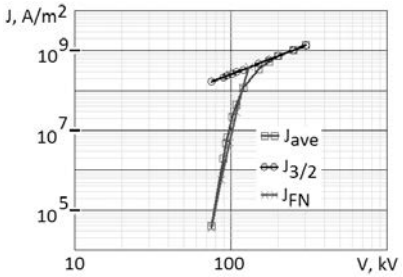

Fig. 10. The averaged current density $J_{ave}(V_C)$ as a function of the cathode applied voltage V_C and its approximation by the Fowler-Nordheim the Child-Langmuir laws

CONCLUSIONS

In this paper we have studied numerically the electron beam dynamics in the high-current diode with a blade-like cathode, which operates in the field emission regime. The computer simulations were performed by particle-in-cell method in the electrostatic approximation. It is shown that there are two modes of diode operation. In the first operation mode the space charge in the diode gap is insignificant. In this case the anode current is small, and its value is determined by the Fowler-Nordheim law. This mode, with increasing potential difference between the cathode and the anode, passes into a mode of the space charge limited diode current. In this case the anode current is determined by the Child-Langmuir law. It is shown that the electron energy distribution function at the anode is almost monochromatic, with a maximum, which is determined by the potential difference between the cathode and the anode. Spatial electron distribution function is significantly expanded compared with the thickness of the cathode due to the topography of the electric field and space charge forces.

REFERENCES

1. O.V. Batishchev, V.I. Golota, V.I. Karas', et al. Linear induction accelerator of charge-compensated ion beams for ICF // *Plasma Phys. Rep.* 1993, v. 19, № 5, p. 611-646.
2. V.I. Karas', V.V. Mukhin, A.M. Naboka, et al. About compensated ion acceleration in magnetoisolated systems // *Sov. J. Plasma Phys.* 1987, v. 13, № 4, p. 281-283.
3. N.G. Belova, V.I. Karas', Yu.S. Sigov. Numerical simulation of charged particle beam dynamics in axial symmetric magnrtic field // *Sov. J. Plasma Phys.* 1990, v. 16, № 2, p. 209-215.
4. V.I. Karas', N.G. Belova. Acceleration and stability of high-current ion beams in two accelerating gaps of a linear induction accelerator // *Plasma Phys. Rep.* 1997, v. 23, № 4, p. 328-331.
5. O.V. Bogdan, V.I. Karas', E.A. Kornilov, O.V. Manuilenko. 2.5-dimensional numerical simulation of a high-current ion linear induction accelerator // *Plasma Phys. Rep.* 2008, v. 34, № 8, p. 667-677.
6. O.V. Bogdan, V.I. Karas', E.A. Kornilov, O.V. Manuilenko. Numerical simulation of high-current ion linear induction accelerator with additional electron beam injection // *Problems of Atomic Science and Technology. Ser. «Nuclear Physics Investigations»*. 2010, № 2(53), p. 106-110.
7. V.I. Karas', O.V. Manuilenko, V.P. Tarakanov, O.V. Federovskaya. Acceleration and stability of a high-current ion beam in induction fields // *Plasma Phys. Rep.* 2013, v. 39, № 3, p. 209-225.
8. O.V. Manuilenko. Dynamics of the short high-current electron and ion bunches in the peaked fence magnetic field: 2d3v PIC simulation // *Problems of Atomic Science and Technology. Ser. «Nuclear Physics Investigations»*. 2012, № 3(79), p. 183-187.
9. O.V. Manuilenko. Acceleration of the short high – current compensated ion bunches in the peaked fence magnetic field with additional space charge compensation by thermal electrons: 2D3V PIC simulation // *Problems of Atomic Science and Technology. Ser. «Plasma Physics»*. 2013, № 1(83), p. 146-148.
10. J.P. Verboncoeur, A.B. Langdon, N.T. Gladd. An object-oriented electromagnetic PIC code // *Computer Physics Communications.* 1995, v. 87, p. 199-211.
11. R.H. Fowler, L.W. Nordheim. Electron Emission in intense electric fields // *Proceedings of the Royal Society of London. Series A.* 1928, v. 119, p. 173-181.

12. L.W. Nordheim. The effect of the image force on the emission and reflection of electrons by metals // *Proceedings of the Royal Society of London. Series A*. 1928, v. 121, p. 626-639.
13. М.И. Елинсон, Г.Ф. Васильев. Автоэлектронная эмиссия / Под ред. Д.В. Зернова. М.: Гос. изд. физ.-мат. лит. 1958, 272 с.
14. Ненакаливаемые катоды / Под ред. М.И. Елинсона. М.: Сов. радио, 1974, 336 с.
15. G.A. Mesyats. *Ectons*. Part I. Ekaterinburg: "Nauka", 1993, 184 p.

Article received 25.05.2015

КОМПЬЮТЕРНОЕ МОДЕЛИРОВАНИЕ СИЛЬНОТОЧНОГО ДИОДА: ОТ АВТОЭЛЕКТРОННОЙ ЭМИССИИ К ОГРАНИЧЕНИЮ ТОКА ПРОСТРАНСТВЕННЫМ ЗАРЯДОМ

О.В. Мануйленко, В.И. Карась, Е.А. Корнилов, В.А. Винокуров, В.С. Антипов

Представлены результаты численного моделирования динамики электронного пучка в сильноточном диоде с ножевым катодом, который работает в режиме автоэлектронной эмиссии. Численные моделирования были выполнены методом макрочастиц в электростатическом приближении. Показано, что существуют два режима работы диода. В первом режиме пространственный заряд в диодном промежутке мал. В этом случае анодный ток невелик, а его величина определяется законом Фаулера-Нордгейма. Этот режим при увеличении разности потенциалов между катодом и анодом переходит в режим ограничения тока диода пространственным зарядом. И тогда анодный ток определяется законом Чайлда-Ленгмюра. Показано, что функция распределения электронов по энергии у анода практически монохроматична, с максимумом, определяемым разностью потенциалов между катодом и анодом. Функция распределения электронов в пространстве значительно уширена по сравнению с толщиной катода, что объясняется топографией электрического поля в исследуемой системе и действием сил объемного заряда.

КОМП'ЮТЕРНЕ МОДЕЛЮВАННЯ ПОТУЖНОСТРУМОВОГО ДІОДА: ВІД АВТОЕЛЕКТРОННОЇ ЕМІСІЇ ДО ОБМЕЖЕННЯ СТРУМУ ПРОСТОРОВИМ ЗАРЯДОМ

О.В. Мануйленко, В.І. Карась, Є.О. Корнілов, В.О. Вінокуров, В.С. Антіпов

Представлено результати чисельного моделювання динаміки електронного пучка в потужнострумовому діоді з ножовим катодом, який працює в режимі автоелектронної емісії. Чисельні моделювання були виконані методом макрочастинок в електростатичному наближенні. Показано, що існують два режими роботи діода. У першому режимі просторовий заряд у діодному проміжку малий. У цьому випадку анодний струм невеликий, а його величина визначається законом Фаулера-Нордгейма. Цей режим при збільшенні різниці потенціалів між катодом і анодом переходить у режим обмеження струму діода просторовим зарядом. У цьому випадку анодний струм визначається законом Чайлда-Ленгмюра. Показано, що функція розподілу електронів за енергією біля анода практично монохроматична, із максимумом, який визначається різницею потенціалів між катодом і анодом. Функція розподілу електронів у просторі значно розширена порівняно з товщиною катода, що пояснюється топографією електричного поля в досліджуваній системі і дією сил об'ємного заряду.